

Modelling II

Modeling of Ultrasonic Testing for Inspection of Nodular Cast Iron Insert

J. Pitkänen, Posiva Oy, Finland; M. Sarkimo, VTT, Finland; S. Lonne, CEA, France

ABSTRACT

Nodular cast iron insert will be used as the inner component of nuclear fuel disposal canister. The outer cover of the canister is copper tube of 50 mm nominal thickness. Nodular cast iron insert is cast around several steel channels, which also strengthen the structure. The mechanical properties of the cast iron insert will be tested according EN-1563 /1/. According the specifications 100% NDT should be carried out for the insert in order to detect possible defects. The standard EN-12680-3 /2/ describes ultrasonic testing of nodular cast iron components and it can be used when applicable. For practical application of ultrasonic inspection the cast iron insert has been divided to following zones.

- Surface zone
- Near surface zone
- Zone between steel channels
- Nearest corner area zone

Each zone will be tested with different ultrasonic techniques. All of these techniques have been also modeled to optimize ultrasonic inspection. The preliminary acceptance criteria have been computed for these zones. Several defect types have been assumed in the acceptance criteria computations.

Surface zone will be tested with TRL 70° 2MHz probes. Here surface defects (notches) and side drill holes were used as reference reflectors. The modeled and measured indications from the notches predict clear reflection possibility from the notch tip. This indicates good sizing capability of the probe for surface defects.

The near surface zone will be tested with 2 MHz normal linear phased array probe with 112 elements. For the detectability of slag inclusion was referenced to side drill holes. The simulation results were compared to defect indication from the reference specimen KLM 125.

The zone between steel channels is inspected applying two phased array consisting 32 elements. The frequency of the probes was 1 MHz. Simultaneously both pulse-echo mode of both probes and transmission mode through the insert are applied.

The nearest corner area zone includes the volume around the fuel channel corner that is nearest to the outer surface of the insert and it has in practice minimum thickness of 35 mm. This zone will be inspected with 3 MHz 48 elements phased array probe. The corner inspection is made to detect possible oxide inclusion, which can be origin to crack type of defects. With actual configuration some ultrasonic modeling using variable notch depths was carried out. Also experimental measurements were performed applying various notch depths at the channel corner.

MANUFACTURING NODULAR CAST IRON INSERT

The parts of cast iron insert are: steel profile cassettes and cast nodular iron base. Steel profile cassettes will be manufactured of material according to the standards EN 10025 S355J2G3; SS 14 2172 or similar /3, 4/ and the cast nodular iron have to fill up the requirements of Grade EN-GJS-400-15U according to EN 1563 /1/. During the manufacturing the steel profile cassettes are connected to each other with support plates in order to hold the structure during casting. Several of these support plates are welded at symmetrically in circumference direction and with equal-distances along the axial direction. The steel cassettes are filled with sand in order to keep the steel cassettes straight. The straightness of the steel cassettes will be also gauged during assembly of the mould for the casting. The corner radius as well the position of the corners can affect to the stress concentration of the manufactured nodular cast iron insert. Several measures are gauged according to the manufacturing specification, which are not relevant for the NDT even though some measures can be statistically measured from mechanized ultrasonic testing throughout the whole insert component like the

distances and positions of the steel cassettes corners from the surface. These items will be discussed more thoroughly in other publications /5, 6, 7, 8, 9/.

During casting the proper melt temperature are still studied and used temperatures are between 1310 – 1370 °C. The casting takes about 1 minute to fill the mould Figure 1 /9/.



Figure 1 - Casting of nodular cast iron insert (left) and finally machined cast iron insert (right)

The designs of Finnish cast iron insert are shown in Figure 2 /10/. All different designs have also different lengths. The EPR insert has about 5 m length and weight 18 tons, VVER is the shortest in length about 3,4 m and in weight 10 tons. BWR type insert like in Olkiluoto I and II has length about 4,5 m and weight 13 tons.

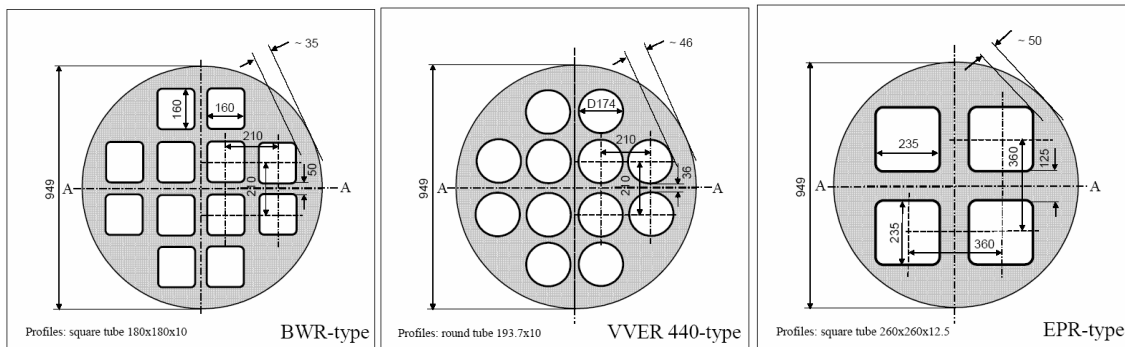


Figure 2 – Design of different Finnish cast iron inserts

DEFECT TYPES IN CAST IRON INSERT

Microstructure of nodular cast iron reveals several defect types like blowholes, pinholes, slag inclusions and their agglomerates, but also oxide filled cracks, variations in graphite nodularity, areas with clustered graphite and/or with deleted graphite. These defect types are discussed in the publications 6 and 7.

Shrinkage Cavity

Shrinkage cavity is irregular cavity inside the cast. The wall of the cavity is often filled with dendrites. In the cast has been local temperature Centrum and no metal has been cast in that area. Shrinkage cavities can be detected in ultrasonic testing, Figure 3 /5/.

Shrinkage Pores

Shrinkage pores can be detected visually, Figure 3 /6/. The shrinkage pore occurs in limited areas in castings. Crystal growth is such that it has developed pores not cavities. In those areas the ductility and strength of material is lowered. Shrinkage pores can be detected in ultrasonic testing.

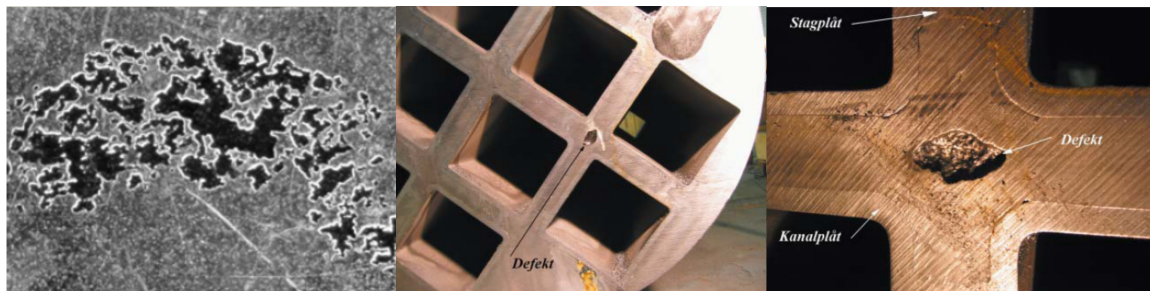


Figure 3 - Micrograph of shrinkage pore (on the left) and shrinkage cavity (on the right)

Blow hole

The gas from the liquid of cast quite often in connection to some central core in the cast forms blowholes. The dimensions of the blowhole vary about from 2 mm to 20 mm. Same situation can be in nodular cast iron inserts the gas formation connections to cassettes, Figure 4 /7/. Blowhole lowers the strength of material. Blowholes can be detected in ultrasonic testing.



Figure 4 - Blowhole defects in the cast iron insert

Pin hole

Pinhole forms on the surface of the cast specimen. The dimension of the pinhole is about from 1 mm to 100 mm it can be open to the surface or closed. Pinhole is in general without any coating in the inner surface of the defect. Pin hole can be caused by gas closed in the cast. Pin hole can be detected in ultrasonic testing.

Slag, oxide or sand grain inclusions

Slag inclusions in nodular cast iron forms often from a dark or black slag particle, which dimension is about 1 mm and it occurs on fracture surfaces or on the machined surface. Very often nearest graphite is lamellar. Slag forms often magnesium oxide, -sulphide or only enriched magnesium slag from casing. These defects are normally detected in metallographic samples but not in ultrasonic testing. Sand grains can be either on the surface or inside of the castings, Figure 5 /6/. The sand in the mould or the parts of mould is not necessarily to detect in ultrasonic testing,

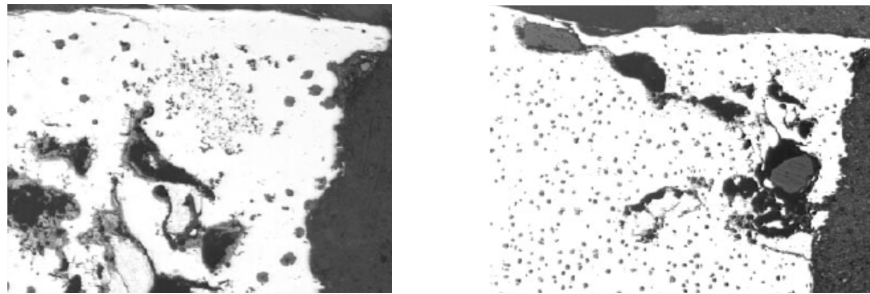


Figure 5 - Micrograph of slag inclusions is shown on the left and Micrograph of sand grain in casting on the right /6/.

Elephant skin

On the surface of the casting is detectable round, in one direction stretched cavity, which look like wrinkled skin like elephants have. These stretched cavities have a certain regular form on the surface. This form can occur against form surface because of ductile thin coating on the upwards-ascending liquid iron.

Cracks

For the cast iron insert was carried out pressure test in JRC Petten /12/. The computed pressure these insert should be able to resist is 44 MPa. In these tests the insert collapsed at about 3 times required pressure (139 MPa). So these inserts showed remarkable toughness against high pressure.

During these tests cracks initiated in the neighborhood of steel channels into the cast material.

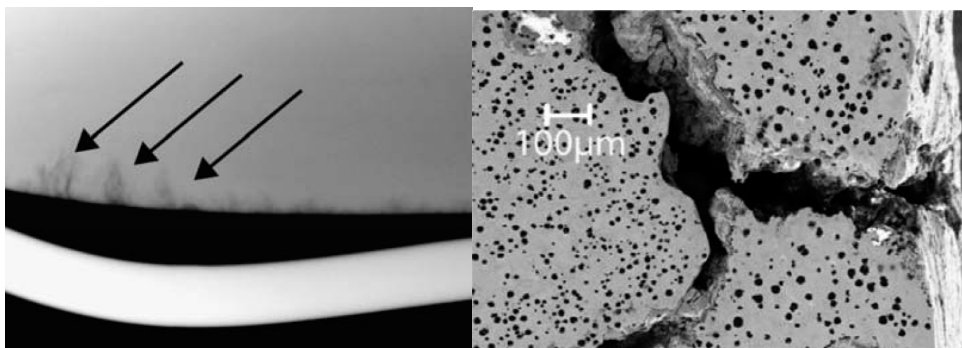


Figure 6 - On the left in x-ray image is clearly detectable several cracks, which have initiated from the outer surface of the steel channel during the pressures tests. On the right is shown micrograph of one crack /11/

Low Nodularity

The nodularity has been specified because low nodularity can decrease toughness of the structure. In general it has been shown that in ultrasonic inspection changes in nodularity can be detected /12/. In this case also the amount of ferrite has an effect on the sound velocity of the structure. When nodularity is lowered the ferrite content is increased thus they are opposite effects and so it makes more difficult to distinguish changes in the nodularity. The inspection of nodularity is done according to ISO 945 /13/, which means that 80% of the nodules must be class 5 and 6. Additionally there is not allowed to have at all class 1 and 2 structures. In Figure 7 is shown the structure of nodular cast iron insert material /9/.

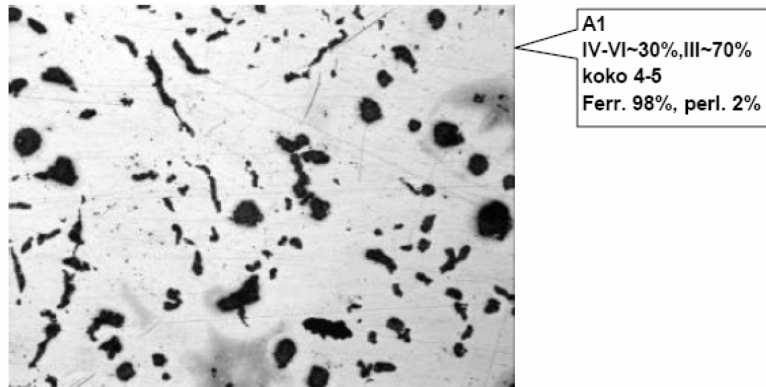


Figure 7 - Sketches of different defect types in the EB-weld /9/.

PRELIMINARY ACCEPTANCE CRITERIA FOR INSPECTION OF INSERTS

To evaluate what could be tolerable defects sizes in inserts for external pressure load computations were carried out by SKB and preliminary allowable defect sizes were produced. The statistical background for these computations were from the co-operation with JRC Petten /13, 14/. Dillström had made previous calculations for insert in publication /13/. In table 1 and 2 is summed the largest allowable planar and volumetric type defects /15/. The size of allowable defect is depending on the location of the defect. The insert has been divided in 4 or 5 categories depending on the location of the inspection area and what type fuel elements should be stored. For each category the allowable defect size has been computed separately /15/. Similar calculations for insert has been computed in /16/. Fault resistance analyses for bending type loads for the insert are under way.

Table 1 - Planar (Crack-like) type of defects (1:6/ height: length)

PWR			BWR		
Zone	Height [mm]	Length [mm]	Zone	Height [mm]	Length [mm]
A	37	222	A	53	318
B1	65	390	B	112	672
B2	50	300			
C	24	144	C	104	624
D	32	192	D	32	192

Table 2 - Volumetric type of defect (round holes through the whole canister)

PWR		BWR	
Zone	Diameter [mm]	Zone	Diameter [mm]
A	40	A	80
B1	60	B	100
B2	20		
C	20	C	100
D	20	D	20

MODELLING WITH CIVA

Theoretical background

Ultrasonic modeling tools have been developed and integrated in the CIVA software platform for NDE /17/, dedicated to simulation and processing of various techniques (UT and ECT in CIVA 8.1 and XR modules in forthcoming CIVA 9 release). For ultrasonic inspections, the modeling codes allow to simulate the response of arbitrary flaws (various shapes: calibration reflectors or more complex shapes arbitrarily located and oriented) inside components of canonical or complex shape (CAD defined for instance). Those components can be made of isotropic or anisotropic materials, and the component's structure can be homogeneous or heterogeneous. Then it is possible to simulate inspections with various probes (contact or immersion, pulse echo or dual RT, single crystal or phased array probes) which radiate Longitudinal and/or Transverse bulk waves, with or without mode conversions occurring at the specimen boundaries or after reflection on the flaw. Simulated data may be displayed using the same format as the UT acquisition data files so as to make easier comparisons between both kinds of data.

CIVA modeling tools include beam propagation and flaw scattering codes based onto semi-analytical approach in order to optimize computation times, as most industrial studies require the modification of one or several parameters for techniques optimization. However, the codes also need to account for realistic configuration; therefore numerical integration is also made to deal with 3D and transient propagation and scattering. Finally, any semi-analytical approach is valid for its own validity range, so that validation of codes (and knowledge of intrinsic limitations) is a key factor of the confidence of the codes. In order to fulfill these requirements, experimental validations of the codes, as well as return of experience from CIVA users, have to be carried out.

To calculate the transient wave field radiated inside the specimen, the transducer is discretized as a series of source points over its surface /17/. For each source point, elementary contributions are obtained by means of the pencil method (a high frequency approximation) /18, 19/. The pencil-matrix formulation allows one to predict wave front radii of curvature along each wave path as well as its time of flight; it is combined with the computation of plane wave transmission/reflection coefficients corresponding to each interaction of the pencil with an interface. Impulse responses are then synthesized from these contributions and convolved with the input signal.

The flaw scattering model is based on three steps: calculation of the incident field over the flaw surface, calculation of the flaw scattering using Kirchhoff's approximation /20/, and calculation of the received signal using the reciprocity principle /21/ to avoid the integration over the probe in reception. Other models can be used in CIVA like models based on the GTD (Geometrical Theory of Diffraction). In this paper, the only model used was that developed under Kirchhoff's approximation.

In echo predictions, the flaw is meshed and the field scattered at each discrete element is obtained from the field incident on this element by applying Kirchhoff's diffraction coefficient (which depends on the incident and observation angles for this element and on the polarity of both the incident and the scattered modes). Then, the total scattered field is computed by summing the contributions from all elements. Finally, the reciprocity principle is used to obtain the output signal of the probe acting as a receiver.

EQUIPMENT USED FOR ULTRASONIC STUDIES

MultiX – full parallel architecture Phased Array-system of M2M was used for the inspection. In this equipment are 128 parallel channels, which can drive normal linear PA-probes or Matrix PA-probes. Some measurements were carried out also with Sumiad multi-channel system. The used scanner is developed by the SKB in Oskarshamn, Figure 8. In this rotator-scanner is possible to inspect full-scale inserts. For the instant calibration so called minirotorator for the test blocks having a short geometry have been developed. If there are needs to check calibration during inspection it is made possible without changing the insert. Same type of material was inspected also by Lofaj et al /21/



Figure 8 - Inspection of calibration block in the minirotorator on the left and both rotator and minirotorator are shown on the right.

INSPECTION POSSIBILITIES AND MODELLED CASES

In the following are described potential ultrasonic techniques, which can be used for measuring the nodular cast iron insert.

For surface inspection are used 70° TRL (Transmission-receiving-longitudinal, 2MHz) probes. This measurement is carried out in direct contact using water as a couplant between inspection specimen and probe. Probes are focused from 5 mm until 40 mm in depth. The focus point is in 20 mm depth. Four main directions for the inspection are used (2 in axial and 2 in circumference directions). This technique is simple method for evaluating the surface volume until the nearest corner of the steel cassettes. The method is time consuming but can be accelerated by increasing the probes and its construction. While the nearest corner area of the steel cassettes is the most critical because of concentration of stresses in extra compression stress state. This can lead to formation of cracks in certain circumstances. In these cases the stress state is far beyond the design pressure. So this area has been inspected with phased array technique using angular scanning with longitudinal waves (3 MHz) from both sides of the corner area as shown in the modeling part. For near surface inspection has been chosen phased array technique with 0° longitudinal wave. The sound path used for inspection is between 20 – 250 mm. The main task is to detect casting defects, which are not between steel cassettes mainly voluminous defect types. Between steel cassettes has been utilized technique, where probe is curved phased array in circumferential direction. Different techniques has been tried for improve the detection of reference reflectors. The optimization of the techniques is still continuing. The used wave type for this inspection is also longitudinal and frequency of the probe 1 MHz. These probe types have been modeled in pulse echo mode. The last technique has been also used for transmission mode with 2 probes and modeling software Civa 8.1 did not provide tools for modeling this type of inspection.

Modeling of surface inspection

The simulation for surface inspection with 70° TRL probes was performed moving the probe along a scan path that crossed the notches at centre. Two cases defect cases with different defect orientations could be simulated. In the first case the orientation of the notches was set normal to the surface. In real

test piece the notches were machined using vertical tool movement when the block was set on its back surface on a horizontal plane. Therefore all the notches (the notches with offset from the centre line) were not normal to the surface. This case could be simulated using defect set-up definition “perpendicular to surface”. The beam of the TRL-probe is applied for the surface and near surface area of inserts and is optimized for the material volume in depth from 5 to 40 mm measured from the outer surface of the insert. The simulation result of the 1, 2 and 4 mm deep notches together with Ø 3mm SDH located at 20 mm from outer surface is shown in the Figure 9.

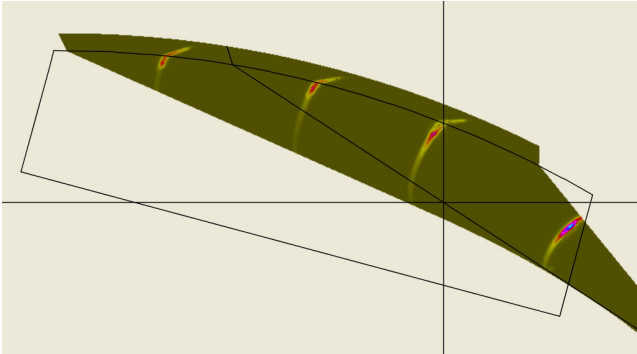


Figure 9 - Simulation result shown as B-scan. The indications from left to right originate from 1, 2 and 4 mm notches and Ø 3mm SDH.

Modeling of near surface inspection

The simulation of the near surface inspection was performed with a 2 MHz 0° phased array probe. The real probe applied in the experimental measurements has 112 elements and has a total active area of 139.9 mm by 20 mm. During the real experimental measurement electronic scanning was applied. During this scanning 24 elements were activated at a time to produce ultrasonic pulses. In Figure 10 the ultrasonic field produced by 24 elements into insert material is shown in two directions. The amplitude (sound pressure) values were evaluated from the simulation results. The maximum of the amplitudes along the sound field is presented and visualized in Figure 10. Amplitude measurement was performed from simulation result computed both in axial and circumferential directions taking into account maximum. Both transmission and reception are taken into account. The results of echodynamic curves at the centerline of the sound beam axis curves are identical except the very beginning of beam where the beam in axial direction is split.

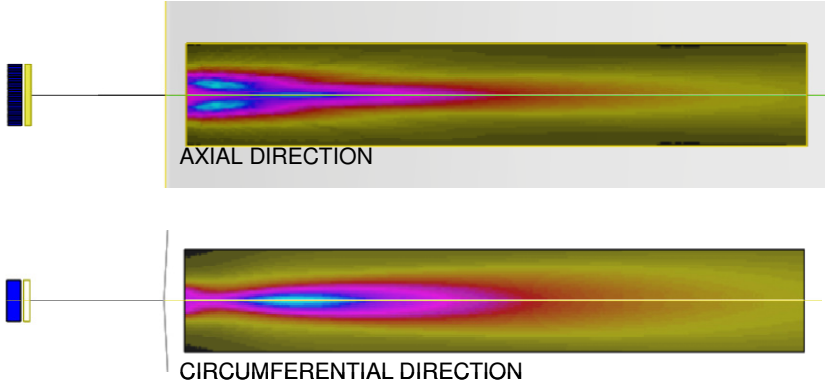


Figure 10 -- Ultrasonic field of the 0° probe when 24-elements of the probe are applied. Sound pressure distribution both in axial and circumferential direction. Two-dimensional computation was applied. The beam 10 - 310 mm below surface is shown.

The beam shape and opening was also analyzed using cross-section taken at different depths. The principle for computation definition of these cross-sections is given in Figure 11. The results for curve are analyzed from the beam widths at different depths shown in the Figure 12.

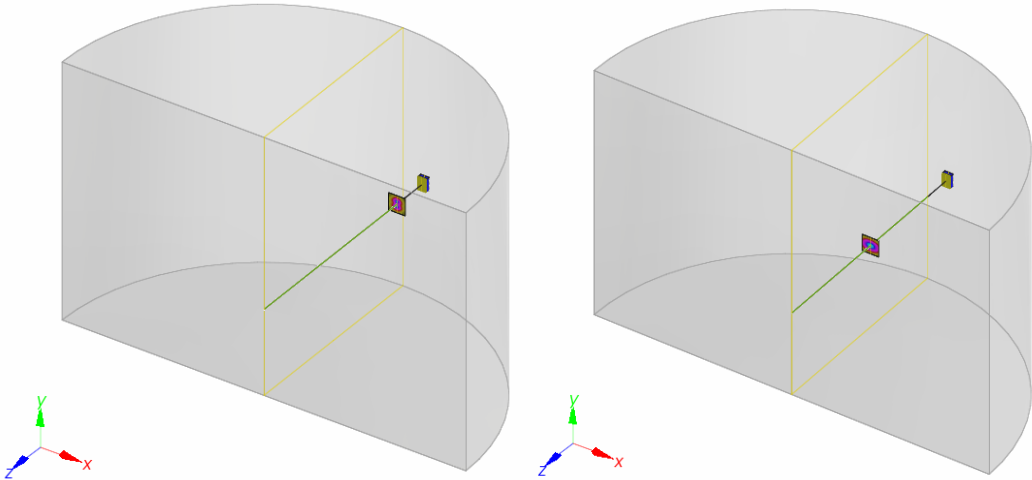


Figure 11 - Computation of the field cross-sections is shown in the picture. The computation planes for two different depths are visualized.

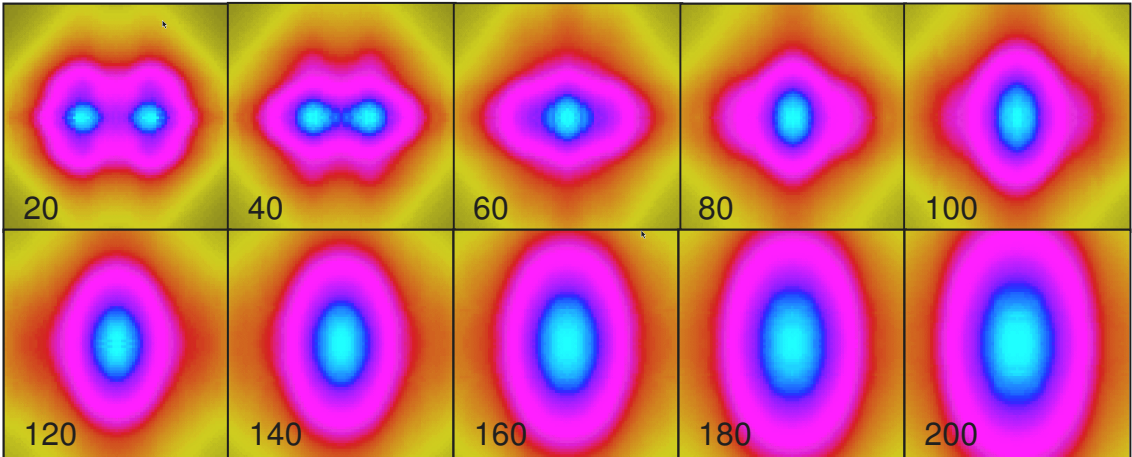


Figure 12 - Field cross-sections at different depths. The horizontal direction of the figure is the axial direction of the insert cylinder. The total area covered by each figure is 50 mm x 50 mm.

Ultrasonic inspection between steel channels

Several ways were tried to model the inspection of area between steel channels. The one way of the beam simulation was performed using focusing. One focus point was set at the distance 125 mm from the surface and all probe elements were used to produce the beam. The beam pattern formed in this case is shown both in circumferential and axial direction is in Figure 13. It can be seen that the beam is more coherent than in the other modeled cases.

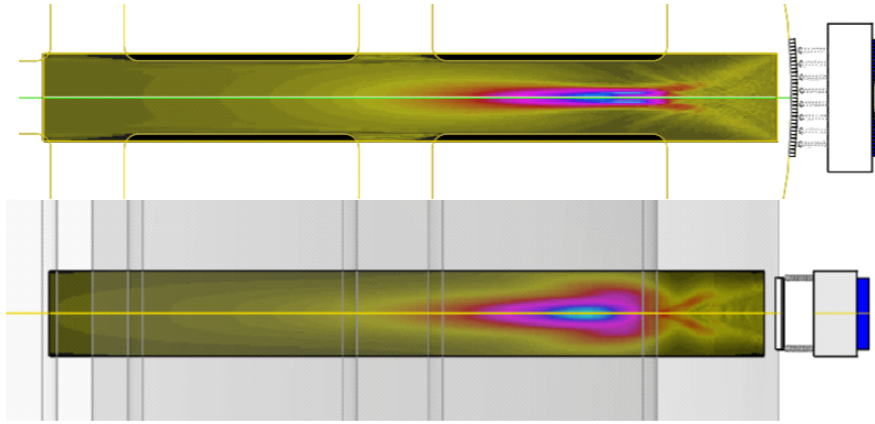


Figure 13 - Ultrasonic beam in the long path when it is focused at 125 mm from the surface. Circumferential (top) and axial (bottom) view of the beam is shown. Modeling was carried out to optimize through-inspection of whole center area of the insert.

The sound pressure variation between the two simulation applications described above is shown in the Figure 14. From the simulation results the amplitude values were measured along the beam centre lines taking into account both transmission and reception. It can be noticed that focusing produces well strong sound beam round the focus point. At very long distances the sector scan is able to produce comparable or even stronger sound field.

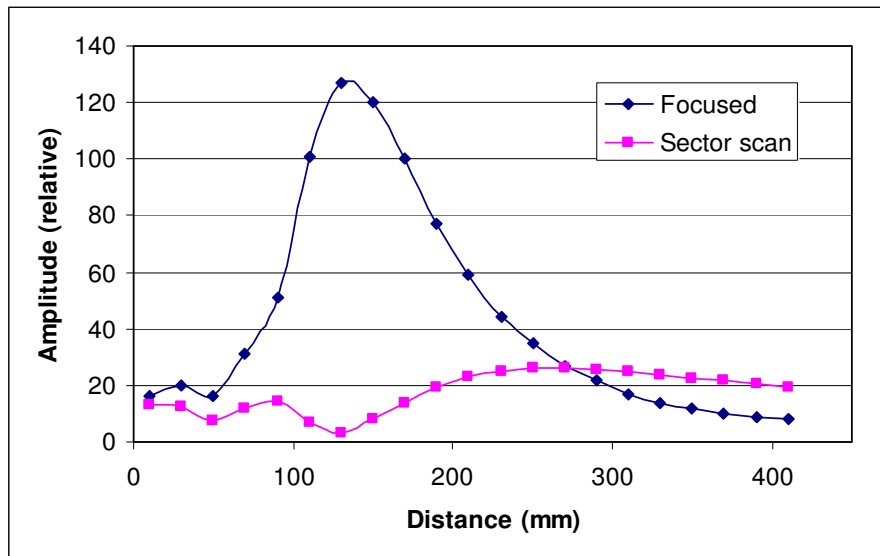


Figure 14 - The relative sound pressure along the field centreline is shown in the long path between the channels. The curves shown are sound field focused at 125 mm and sector scan.

MEASUREMENTS COMPARED TO MODELLING

For the surface inspection the modeled amplitudes were in good agreement with the measured data. The comparison between modeled data of defect orientation is shown in Table 3. From the modeled data was seen clearly that the maximum amplitudes were collected on the tips of the notches, which is more or less diffraction indication. This phenomenon can be used of course for sizing purposes. For sizing the exact position of each A-scan of the probe is very important.

Table 3 - The amplitudes of simulation are given in relation to the amplitude of \varnothing 3mm SDH at depth of 20 mm from outer surface

File: Fe-Calibr_r481_TRL70_f20mm_Tg_0to100_MS.xml			
Defect orientation normal to surface		Defect orientation Perpendicular to surface (real positions)	
Reflector Size / Depth	Amplitude [dB]	Reflector Size / Depth	Amplitude [dB]
SDH \square 3mm	0	SDH \square 3mm	0
Notch 1 mm	-7.3	Notch 1 mm	-5.9
Notch 2 mm	-6.6	Notch 2 mm	-6.2
Notch 4 mm	-6.1	Notch 4 mm	-9.5
Notch 8 mm	-2.7	Notch 8 mm	-2.3
Notch 10 mm	-2.7	Notch 10 mm	-2.0

By the modeling of near surface inspection to be able to compute the simulation with similar manner as the experimental measurement was performed the probe had to be changed to single element configuration. The probe parameters in this simulation were otherwise same as in previous simulations but a single crystal element with the aperture size corresponding to the active aperture size of the phase array probe was applied. The simulation results comparison with the experimental measurement results of the calibration block KLM125 are shown in the Figures 15 and 16. The simulation in this case shows also to be in good agreement with experimental data.

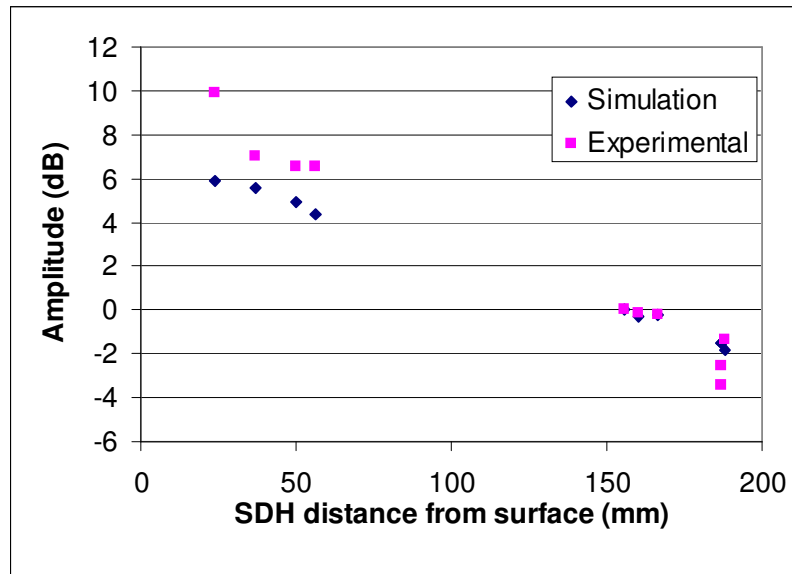


Figure 15 - Comparison of the SDH echo amplitudes from simulation and experimental measurement. SDH at the distance of 155.5 mm is used as reference level for both simulation and experimental measurements (amplitude = 0 dB).

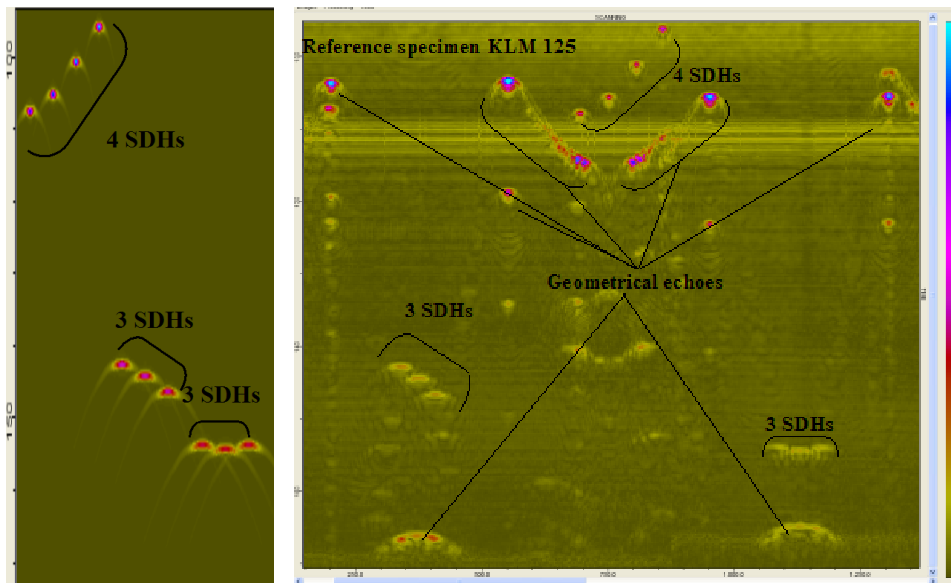


Figure 16 - Modeling results (on the left) are compared to measured data (on the right). The modeled data showed to be similar with measured data. The noise and geometrical echoes from the probe and calibration block KLM 123 is clearly seen in the measured data

SUMMARY AND CONCLUSIONS

In this study was shown the developed ultrasonic inspection techniques for nodular cast iron insert. With help of these techniques the insert can be inspected sufficient extensively. The amount inspection needed will be studied more detailed in the future. The modeling had two functions in the inspections – quick optimization of the techniques and validation of used technique. The phased array technique is complicated and modeling helps simplifies optimization and decreases unnecessary experimental work.

Measurements has been carried out with M2M-equipment (Posiva) and TD-focus Equipment (SKB). The experimental data from the inspections were in good agreement with the modeled data was as shown. The amount of inspections to be carried out in the manufacturing of the insert component for nuclear fuel repository has to be controlled with careful tests and metallurgical verification of indications. For inspection of these inserts the preliminary acceptance criteria were computed and they will be tested in trial phase of manufacturing of different types of inserts

REFERENCES

- 1) EN-1563: 2006+A1+A2, European standard, founding –Spheroidal graphite, CEN, confirmed 2006-01-23, 50p.
- 2) EN 12680-3 Founding – Ultrasonic examination, Part 3: Spheroidal graphite cast iron castings, CEN, confirmed 2003-08-18, 32p.
- 3) EN- 10025-1, Hot rolled product of structural steels, Part 1: General delivery conditions, CEN, confirmed 2004-12-21, 57p.
- 4) EN- 10025-2, Hot rolled product of structural steels, Part 2: Technical delivery conditions for non-alloy structural steels, CEN, confirmed 2004-12-21, 66p.
- 5) SKB, 2006a,, Kapsel för använt kärnbränsle, Tillverkning och förslutning, SKB R-06-01, September, 79p.
- 6) SKB, 2006b, Kapsel för använt kärnbränsle, Tillverkning av kapselkomponenter, SKB R-06-03, September, 67p.
- 7) SKB, 2006c, Kapsel för använt kärnbränsle, Oförstörande provning av kapselkomponenter, SKB R-06-05, September, 51p.

- 8) SKB, 2006d, Ansökan för inkapslingsanläggningen och slutförvaret för använt kärnbränsle, SKB R-06-50, September, 70p.
- 9) Raiko, H., 2003, Test Manufacture of a Canister Insert, Posiva Working Report 2003-59, November 2003 21 p.
- 10) Raiko, H., 2005, Disposal Canister for Spent Nuclear Fuel – Design Report, Posiva Report 2005-02, July 2005, 61p.
- 11) Nilsson, K. -F., Burström, M., Lofaj, F., Andersson, C. -G., 2007 Failure of spent fuel canister mock-ups at isostatic pressure 14 (2007) pp. 47 – 62
- 12) Wilcox, M., 2003, Ultrasonic Velocity Measurements Used to Assess the Quality of Iron Castings, Web: www.InsightNDT.com, 13 p.
- 13) EN-ISO 945: 2006, European standard, Cast iron. Designation of microstructure of graphite (ISO 945), CEN, confirmed 1994-12-05. 12p.
- 14) Nilsson, K. -F., Blagoeva, D. & Moretto, P., 2006, An experimental and numerical analysis to correlate variation in ductility to defects and microstructure in ductile cast iron components, Engineering Fracture Mechanics, 73 (2006) pp. 1133 – 1157
- 15) Dillström, P., 2005, Probabilistic analysis of canister insert for spent nuclear fuel, SKB TR-05-19, October 2005, 37p.
- 16) Pitkänen, J., Leskinen, N., Ryden, H., & Emilsson, G., 2006, Defect types, NDT and preliminary acceptance criteria approach based on the damage tolerance analysis and international standards in the manufacturing of nodular cast iron insert, Workshop on Design and Assessment for Radioactive Waste, 21. – 22. November Bergen JRC, 33p.
- 17) Koyama, T., Zhang, G. & Jing L., 2006, Mechanical integrity of Canister Using a Fracture Mechanics Approach, SKI Report 2006:36, July 2006, 64p.
- 18) More information about CIVA may be found at <http://www-civa.cea.fr>
- 19) Calmon P., Lhémy A., Lecœur-Taïbi I. and Raillon R., “Integrated models of ultrasonic examination for NDT expertise”, in *Review of progress in QNDE*, edited by D. O. Thompson and D. E. Chimenti, Vol. 16B, Plenum Press, New York, 1997, pp. 1861-1868.
- 19) Gengembre N., "Pencil method for ultrasonic beam computation", Proc. of the 5th World Congress on Ultrasonic, Paris, 2003.
- 20) Raillon R. and Lecœur-Taïbi I., “Transient elastodynamic model for beam defect interaction, Application to nondestructive testing”, *Ultrasonics*, 2000 Vol. **38** pp. 527-530.
- 21) Auld B.A., *Wave motion*, 1979 Vol. **1** pp. 3-10.
- 22) Lofaj, F., Seldis, T., Nilsson, K. -F., Eriksson A., 2006., Ultrasonic study of Defects in Ductile Cast Iron Insert for Nuclear Fuel Disposal, ECNDT 2006, 25.-29. September 11p.

Numerical Modeling of Ferromagnetic Tube Inspection via an Integral Equation Approach

A. Skarlatos, G. Pichenot, CEA-LIST, France; D. Lesselier, M. Lambert, B. Duchêne, CNRS –
Supélec – University Paris-Sud, France

ABSTRACT

Maintenance and safety issues in industrial installations are often involved with the demand for reliable inspection of ferromagnetic tubes. For the nuclear industry, this kind of tubes is met primarily in fast neutron reactor installations. The development of efficient software tools for the simulation of such inspection procedures is thus an important task. This contribution presents a Volume Integral Method (VIM) formulation for the modeling of eddy current inspection of ferromagnetic tubes. The model was developed within the framework of the CIVA platform providing an extension of its functionality. It has been validated using experimental results collected by tubes with similar characteristics with those met in fast neutron reactors and is thus suitable for the simulation of this kind of applications. The results of the model are in good agreement with simulations obtained by the Finite Elements Method (FEM).

INTRODUCTION

The Eddy Current (EC) Nondestructive Evaluation (NDE) of ferromagnetic tubes has been developed during the last decades and it is now a standard industrial technique used in various applications. In nuclear energy domain in particular, the inspection of ferromagnetic tubes usually concerns the control of the condensers circuits in sodium-cooled fast neutron reactors. The Remote Field Eddy Current Technique (RFEC) is perhaps the most usual technique in such applications. Even if the latter has been used for many years, there is still a lack of appropriate simulation tools able to accurately and efficiently model this technique. Until now the main tool for numerical modeling of eddy current inspection of ferromagnetic materials was the Finite Elements Method (FEM). However, FEM faces specific drawbacks when studying NDE problems since it requires the discretization of an extended domain even for small defects. Furthermore, the Eddy Current problem has to be solved many times in order to simulate a complete scan of the detection probe.

For these reasons the Volume Integral Method (VIM) formulation seems an interesting alternative to model NDE problems. The EC module of the NDE simulation tool CIVA (a multi-technique dedicated platform with Eddy Current, Ultrasonic and Radiography modules for NDE) is based upon such a formulation [1]. The VIM formulation is already implemented in CIVA for NDE of nonmagnetic materials [2, 3]; we are concerned herein with its extension to the case of ferromagnetic tubes.

In ferromagnetic tubes, the presence of material defects results in a local variation of magnetic permeability in addition to the variation of conductivity met in nonmagnetic materials. Thus, the electric field integral equation, which arises in the nonmagnetic case, has to be combined with a magnetic field integral equation in order to get a well determined problem. This system involves the full family of Green's dyads and leads to an increased computational effort. Although the theoretical formulation developed herein is generic and not restricted to a specific technique, a special attention is paid to the RFEC technique due to its practical importance.

After a brief description of the theoretical formulations used to solve the ferromagnetic configurations, simulation results are presented and validated using experimental data collected by RFEC probes. Comparisons with FEM simulation results are performed as well.